Plasmonics
https://doi.org/10.1007/s11468-024-02537-5

RESEARCH

# Surface Plasmon Resonance Sensor Based on Perovskite Layer and Bimetallic Silver-gold for the Detection of Human Breast Cancer

**Habia Mohamed Ilyes**[1,2] · **Habia Ghania**[3] · **Manallah Aissa**[1] · **Ayadi Khaled**[1]

Received: 16 July 2024 / Accepted: 9 September 2024


## Abstract

Cancer is a leading cause of morbidity and mortality worldwide. Millions of individuals throughout the world suffer from cancer and other illnesses. This is a leading cause of human death each year. Huge efforts were made to develop simple, precise, and cost-effective technologies for detecting various diseases. As the detection of cancer and diabetic disorders has received a lot of interest in the field of biosensing, several methods have been developed to detect these diseases with high accuracy. This study investigates the possibility of surface plasmon resonance (SPR) for human breast cancer detection utilizing a bimetal silver with gold in permutation and hybrid organic–inorganic halide perovskites ($MAPbX_3 \equiv CH_3NH_3PbY_3$, with $M = CH_3$, $A = NH_3$, and $Y = Br$) sensor that operates at a specific wavelength of 633 nm. Early cancer identification is critical for improving patient outcomes, and SPR presents a promising path for label-free, sensitive detection of cancer biomarkers.

**Keywords** Optical sensors · SPR sensor · Perovskite · Cancer detection · Human disease

## Introduction

Cancer is a disease characterized by the uncontrolled proliferation of aberrant cells in a specific section of the body [1]. Cancers are a leading cause of death worldwide (Breast cancer caused 670,000 deaths globally in 2022) [2]. Early diagnosis is crucial for treating many disorders [3, 4]. Normal healthy cells grow and divide in a controlled manner, and their proliferation is limited to a specific cell density [5]. Cancer cells, on the other hand, continue to divide despite their dense population. Normal cells appear homogeneous in size and shape, whereas cancer cells have an irregular shape and a non-uniform size [1]. Cancer cells are larger than normal cells. Fibroadenomas (FAs) of the breast are fibroepithelial tumors that are most common in adolescent women but can be identified at any age. FAs not only cause psychological suffering and lower quality of life but also raise the risk of getting breast cancer over time [6]. The absolute way to detect many types of cancer is to obtain a sample of questionable biological tissue and examine it using an optical technique [7]. Which must be a faster, simpler, and easier tumor detection approach than biopsy. Surface plasmon resonance is now an acceptable method for disease diagnosis; it is used in a wide range of chemical and biosensing applications, including food safety [8], medical diagnostics [9], and drug diagnostics [10], due to their unique characteristics such as the ability to perform real-time detection in a label-free platform [11], high sensitivity, and quick response [12]. Breast cancer is the most commonly diagnosed disease worldwide, accounting for almost two million cases in 2020 [13]. Surgical procedures, such as mastectomy or tumor excision, continue to be the primary treatment for the condition. However, in some tumor forms, minimum operations are used to reduce the risk of long-term organ damage [14]. Perovskite materials have a number of special qualities that make them very useful for raising sensor sensitivity [15]. Perovskites can be tailored for optimal optical absorption, emission, and carrier transport properties by manipulating their structure and composition [16]. This makes it possible to maximize the sensitivity of optical sensors by optimizing the perovskite layer. Organometallic halide perovskites' excellent electron and hole carrying capabilities make them suitable for use in extremely sensitive electrical sensors. When compared to materials based on carbon, their

✉ Habia Mohamed Ilyes
mohamedilyes.habia@univ-msila.dz

[1] Applied Optics Laboratory, Ferhat Abbas University, Setif, Algeria

[2] Mohamed Boudiaf University, Msila, Algeria

[3] Anti-Cancer Center CAC, Setif, Algeria

Published online: 13 September 2024

metallic and crystalline structure enhances sensitivity even further [17]. The use of bimetallic films in SPR sensors has several advantages, including increased sensitivity, optimal performance through careful thickness management, and the ability to customize sensor features to specific applications [18]. Bimetallic films, such as those made of gold and silver, offer a considerable increase in RI (RI) sensitivity over single metal films. This is principally owing to the combined optical characteristics of the two metals, which boost the evanescent field at the analyte-metal interface, making it more sensitive to changes in the RI of the surrounding medium [19]. The placement of the metal active film on the prism is critical to the performance of SPR sensors. The sensitivity, angular shift, and overall effectiveness of the sensor are all strongly affected by the configuration chosen, such as Prism/Au (gold) or Prism/Ag (silver) [20]. Here is a full comparison between these two configurations. The SPR sensor with a perovskite layer and a bimetallic silver-gold arrangement stands out for its increased sensitivity and figure of merit, cost-effectiveness, adaptability, resilience, and possible integration with advanced sensing technologies. These benefits make it a promising tool for the early identification and surveillance of human breast cancer [21].

Optical detection techniques have their strengths and weaknesses, and the SPR is notable for its ability to provide real-time unlabelled detection of cancer biomarkers, this makes it particularly suitable for early diagnosis of breast cancer. Its versatility and non-invasive nature further enhance its appeal in clinical settings, positioning it favorably compared to other optical detection methods. Comparison with other techniques is represented in Table 1.

## Theoretical Model

Kretschmann's configuration-based optical transduction approach was used to translate changes in the RI at the sensor surface into usable electrical signals [40]. The proposed detector consists of five layers: BK7 prism, silver, perovskite, and a sensing layer for detecting breast cancer cells. The thicknesses of silver, perovskite, and layers are denoted as d1, d3, and d2; the RI are denoted as n1, n3, and n2 respectively. Figure 1 depicts a schematic of a proposed SPR biosensor based on layers of Ag and perovskites. The RI of silver and perovskite (MAPBr3) are presented in Table 2. The coupling between incident light and SPs at the metal-dielectric contact is as follows [41].

$$\frac{\omega}{c} n_p \sin\theta_{SPR} = real\left(\frac{\omega}{c}\sqrt{\frac{\varepsilon_m n_s^2}{\varepsilon_m + n_s^2}}\right) \tag{1}$$

**Table 1** Comparison of the most techniques used to detect breast cancer

| Optical sensing system | Fabrication steps | Analytical performance |
|---|---|---|
| Fiber optic probe | - Create an optical fiber needle probe with a core diameter of 200 to 600 µm [22]<br>- Precision machining to ensure biocompatibility [23]<br>- Setup of optical components for fluorescence detection [24] | - Supports real-time fluorescence detection [25]<br>- Minimizes unneeded biopsies by confirming the existence of cancer cells [25] |
| SPR | - Production of prisms and plasmonic waveguides [26]<br>- Use of metals (gold, silver, etc.) to improve sensitivity [27]<br>- Calibration to detect specific biomarkers [28] | - High sensitivity, with limits of detection as low as 100 µM for certain analytes [29] |
| Near-infrared (NIR) opti-scan probe | - Creation of an NIR probe for breast tissue imaging [30]<br>- Optimize wavelength selection based on tissue composition [31]<br>- Integration of machine learning models for data analysis [32] | - Effectively assesses cancer burden after chemotherapy [33]<br>- Offers real-time monitoring [32] |
| Colorimetric biosensor | - The use of colorimetric techniques for detection [34]<br>- The creation of sensor surfaces with particular coatings [35]<br>- Sensitivity and specificity tests [35] | - Limit of detection is approximately 160 pg/mL [36]<br>- Effective for the quick detection of cancer biomarkers [37] |
| Optical coherence tomography (OCT) | - The assembly of optical components for coherence detection<br>- Calibration and test for tissue imaging [36]<br>- Integration of imaging software for analysis [38] | - Non-invasive imaging for high-resolution tissue characterisation [39]<br>- Effective for early cancer detection [38] |

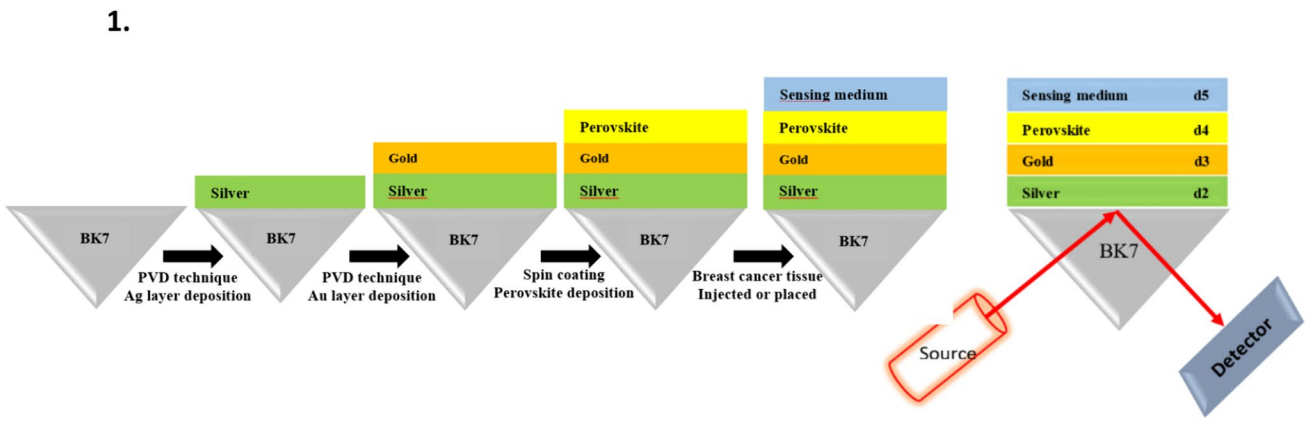


**Fig. 1** Schematic of possible fabrication technique for deposition of various layers sensor construction of the proposed SPR-based sensor utilizing bimetal and perovskite

**Table 2** Dielectric constant values of layers at λ 633 nm

| The used layer | RI (RI) | Ref |
|---|---|---|
| BK7 | 2.2957 | [42] |
| Silver | −18.295 + 0.48085i | [43] |
| Gold | −11.753 + 1.2596i | [44] |
| perovskite (MAPBr3) | 2.008 + 0.0013i | [12] |
| Sensing medium: breast cells | | |
| Normal | 1.7988 + 0.0224i | [7] |
| Cancer | 1.8337 + 0.0156i | |
| Fibroadenoma | 1.7705 + 0.0152i | |

In this equation, np represents the prism's RI, ω represents the incident light's angular frequency, c represents light velocity in a vacuum, εm represents the silver metal layer's dielectric constant, and ns represents the RI of the sensing medium. In this case, the developed SPR biosensor is estimated to operate with a P-polarized wave at a wavelength of 633 nm. When the coupling condition is met, the SPR curve exhibits a narrow dip at the resonance angle ($\theta_{SPR}$) [45]. This angular position experiences a shift ($\Delta\theta_{SPR}$) when there is a small change in the sensing medium value (i.e., Δns) [46]. The sensing performance of an SPR-based sensor is generally evaluated in terms of angular sensitivity (S) full width at the high middle (FWHM) and figure of merit (FOM). These parameters are expressed as follows [47]:

$$S = \Delta\theta_{res} / \Delta n_{sensing} \tag{2}$$

$$FWHM = \frac{1}{2}(\theta_{\max} + \theta_{\min}) \tag{3}$$

$$FOM = S/FWHM \tag{4}$$

To calculate reflectance (R) for p-polarized incident light, the N-layer transfer matrix approach is utilized. This procedure is extremely exact because no approximations are used. MATLAB software was used to compute the analogy of SPR modification. For a multilayer structure, the input of each layer at amplitudes equivalent to a distance z in the layer. The medium layer is described by its RI (nk), permeability (μk), dielectric constant (εk), and thickness (dk). The relationship between the tangential field at the first boundary ($z = z_1 = 0$) and the final boundary ($z = z_{n-1}$) is stated as [48]:

$$\begin{bmatrix} H_{yk}^{0} \\ -E_{xk}^{0} \end{bmatrix} = M_k \begin{bmatrix} H_{yk}(z) \\ -E_{xk}(z) \end{bmatrix} \tag{5}$$

where $H_{yk}^{0}$ and $E_{xk}^{0}$ are respectively the tangential components of the electric and magnetic fields at the boundary of the first layer. $H_{yk}(z)$ and $E_{xk}(z)$ are the fields corresponding to the $N^{th}$ layer boundary. Here, $M_k$ is known as the characteristic transfer matrix of the combined structure and is given by [49]:

$$M = \prod_{k=1}^{N-1} M_k = \begin{bmatrix} M_{11} & M_{12} \\ M_{21} & M_{22} \end{bmatrix} \tag{6}$$

Or, M11, M12, M21, and M22 are the components of the transfer matrix, with [41]:

$$M_k = \begin{bmatrix} \cos\beta_k & -i\sin\beta_k/q_k \\ -iq_k\sin\beta_k & \cos\beta_k \end{bmatrix} \tag{7}$$

$M_k$ named the characteristic matrix for the k-layer and related to the optical properties and the thickness of each layer ($d_k$) where [41]:

$$q_k = \left(\frac{\mu_k}{\varepsilon_k}\right)^{1/2} \cos\theta_k = \frac{(\varepsilon_k - n_0^2 \sin^2\theta)^{1/2}}{\varepsilon_k} \tag{8}$$

$$\beta_k = \frac{2\pi}{\lambda} n_k \cos\theta_k (z_k - z_{k-1}) = \frac{2\pi}{\lambda} d_k (\varepsilon_k - n_0^2 \sin^2\theta)^{1/2} \quad (9)$$

Here $n_0$ mean $n_p$ prism (the RI of prism) the incident level of the system. The reflectivity (R) for incident light is represented as [41, 49]:

$$r_p = \left[ \frac{(M_{11} + M_{12}q_k)q_1 - (M_{21} + r_{22}q_k)}{(M_{11} + M_{12}q_k)q_1 + (M_{21} + M_{22}q_k)} \right] \quad (10)$$

The reflection coefficient ($r_p$) of an incoming light is determined using the reflectivity (R) parameters and is provided by the relation [41, 49]:

$$R = |r_P|^2 \quad (11)$$

## Results and Discussion

This study investigates an SPR structure-based photodetector for detecting cancer and fibroadenoma cells. According to the previous section, the RI of the layers are calculated at 633 nm. Initially, the silver and gold layer thicknesses ($d_{Ag}$, $d_{Au}$) are optimized to yield the lowest possible reflectance or the minimum reflection intensity ($R_{min}$) at resonance, and knowing more structure provides the best sensitivity. This optimization plays an important role in the evanescent field strengthening. Considering normal breast cells, different thicknesses of silver and gold are used for reflectance analysis. In the case of a conventional sensor, the silver thickness is 42 nm and the gold thickness is 40 nm; therefore, in the case of a bimetal sensor, the silver layer is 42 nm and the gold layer is 5 nm. In the other case, gold-silver is raised at 43 and 4 nm respectively, while the thickness of perovskite is chosen at $d_4 = 3$ nm.

Next, the effect of changing the RI of the sensing medium between normal cancer human breast cells on the reflectivity of all six structures SPR designs was investigated. This change in the sensing medium's RI manifests itself as a shift in the resonance angle ($\Delta\theta_{rés}$) of the resonant peak, as shown in the reflectivity vs incident angle curves.

We begin by presenting the proposed SPR sensor-prism/Ag/sensing medium, which achieves a resonant dip in reflectivity of 09.52% at an angle of 68.69° in the reflectance spectra for normal breast cells, as shown in Fig. 2a. Next, the RI of the sensing medium was changed by using cancer breast cells to measure the effect of this adjustment on the position and reflection intensity of the resonance dip. The sensing medium RI changes from 68.69° to 70.25°, resulting in a 1.56° shift in the angular position of the resonant dip with FWHM of the resonance rise from 3.6° to 3.3°. Increasing the RI of a sample leads to increased reflection intensity of the resonant dip, as shown in Fig. 2a, because normal cells have a higher imaginary permittivity than cancer cells. The sensitivity is obtained as 120.55 deg/RIU at optimum conditions. The same behavior is observed in Fig. 2b when we examine the second structure of the sensor, prism/Au/sensor medium. Their resonance angles are 72.83° and 74.75°, corresponding to minimum reflectance ($R_{min}$) of 0.13% and 0.001% for normal and cancer breast cells.

The shift in the angular position of the resonant well and a change in the FWHM of the resonance slope from 9.8° to 9.1°, respectively as presented in Fig. 2b. These values confirm that the FWHM is related to the imaginary part of the propagation vector of surface plasmons in Eq. (12), as imaginary values of metal gold and sensing medium are great and create a big FWHM [50].

$$\mathrm{Im}(k_{sp}) = (\omega/c) * (\widetilde{\varepsilon}_{metal}\varepsilon_{cells}/\widetilde{\varepsilon}_{metal} + \varepsilon_{cells})^{3/2}(Im(\varepsilon_{metal}/Re(\varepsilon_{cells})) \quad (12)$$

The value of $R_{min}$ is very small due to the high imaginary dielectric constant of gold, which depicts the absorption, or the loss of energy at the angle of resonance. The optimal settings result in a sensitivity of 148.52 degrees per RIU. To improve the sensitivity of the sensor for breast cancer detection, another structure is proposed based on the usage of two metals stratified alternatively. The reflection spectra curves in Fig. 2c show the third recommended sensor structure, prism/Ag/Au/sensing medium. When the sensitivity is raised to 112.05 deg/RIU, the $R_{min}$ rises between 20.89 and 13.85% for normal and cancer cells, corresponding to resonance angles of 69.91° and 71.63°, with FWHMs of 4.2° and 3.9°, respectively. In the fourth structure (Fig. 2d), the metals were permuted, resulting in 2.70% intensity for normal cells and 1.06% intensity for cancer cells at the resonance angle. This corresponds to FWHM 7.3° and 7.1°, respectively, with a shift angle of $\Delta\theta res = 1.85°$ and a sensitivity of 142.96 deg/RIU. The bimetallicity plays a greater role in improving the FWHM because it reduces the imaginary part of the surface plasmon vector "ksp" rather than the intrinsic sensitivity of metallic arrangements such as gold and silver.

To enhance the performance of the optical sensor for the detection of human breast cells, an element was put above the metal bimetallic such us perovskite this element presents a high real permittivity and lower absorption described by a small imaginary part of permittivity which can strongly improve the performance of the sensor. Figure 2e shows structure 5 (Prism/Ag/Au/Perovskite/Sensing medium), and the reflectance spectra curves show an offset resonance angle of 1.89° caused by a change in resonance angle between 71.58° and 73.47°, which corresponds to a minimum reflectance intensity of 18.74 to 12.60% for normal and cancerous breast cells. With a FWHM of 4.8° to 4.3° respectively, reaching a sensitivity of 146.05 deg/

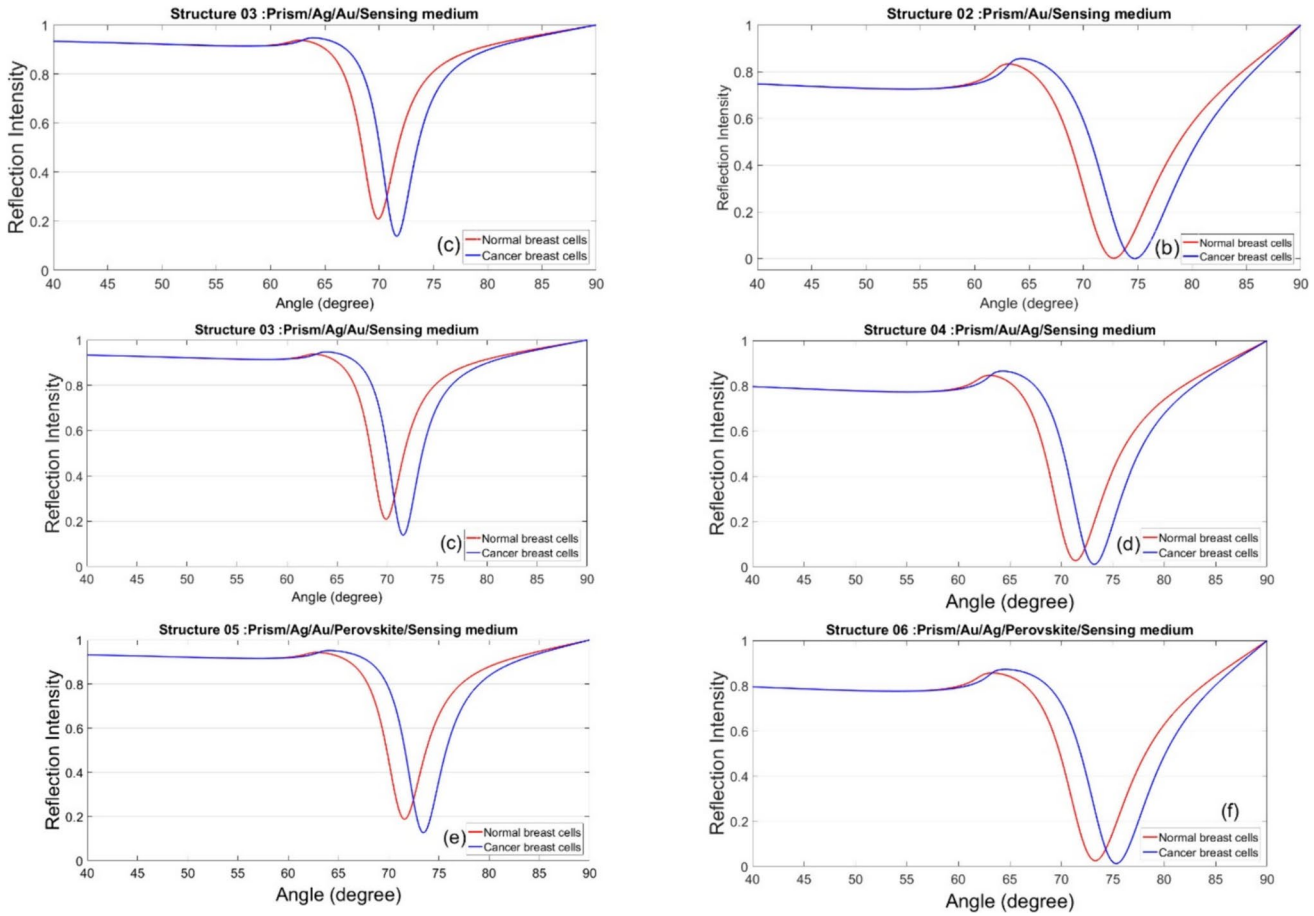


**Fig. 2** **a–f** Reflectance spectra for different structures of suggested SPR with normal and cancer breast cells

RIU. On the other hand, structure 6 of the detection medium suggested by the Prism/Ag/Au/Perovskite/Sensing sensor shown in Fig. 2d illustrates the changes in the resonance angle caused by the variation of the RI of the detection medium of 73.32° and 75.41° creating a displacement angle equal to 2.09°. The FWHM also changes with this case between 8.7° and 8.0° producing a pre-sensitivity of 162 deg/RIU. According to this long study, it is noted that the perovskites layer element helps to improve the sensitivity of the sensor especially if it is coupled with a bimetallic "gold + silver" layers arrangement, which is noteworthy and presented in Table 3, which qualifies it as a good fast cancer cell sensor.

Structure 6 (Prism/Au/Ag/Perovskite/Sensing medium) has the maximum sensitivity at 161.81 deg/RIU, thanks to the bimetallic Au/Ag arrangement and perovskite layer. Structure 1 (Prism/Ag/Sensing Medium) has the narrowest FWHM at 3.3°, indicating precise detection. However, its sensitivity is lesser compared to other structures. Structure 5 (Prism/Ag/Au/Perovskite/ Sensing medium) has the highest merit factor (FOM) of 34.02, which combines good sensitivity with a tolerable FWHM. FOM is a reliable overall

**Table 3** the change in the position of the resonant dip (Δθrés in degrees) and sensitivity are due to a change in the RI of normal and cancer cells of all structures

| | | Δθrés | Sensitivity | FWHM | FOM |
|---|---|---|---|---|---|
| Structure 1 | Prism/Ag/Sensing medium | 1.56° | 120.55 | 3.3° | 36.53 |
| Structure 2 | Prism/Au/Sensing medium | 1.92° | 148.52 | 9.2° | 16.14 |
| Structure 3 | Prism/Ag/Au/Sensing medium | 1.72° | 112.05 | 3.9° | 28.73 |
| Structure 4 | Prism/Au/Ag/Sensing medium | 1.85° | 142.96 | 7.1° | 20.13 |
| Structure 5 | Prism/Ag/Au/Perovskite/Sensing medium | 1.89° | 146.30 | 4.3° | 34.02 |
| Structure 6 | Prism/Au/Ag/Perovskite/Sensing medium | 2.09° | 161.81 | 8.0° | 20.22 |

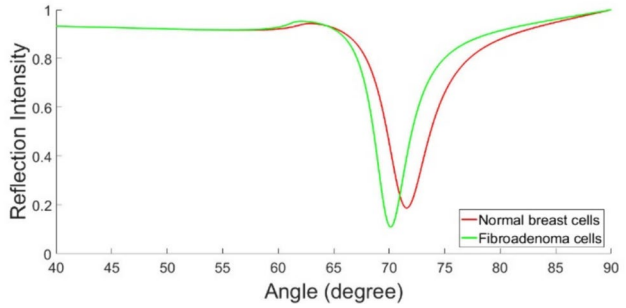


**Fig. 3** Reflectance spectra for the suggested SPR with normal and fibroadenoma breast cells

measure of sensor performance. Therefore, we can show that structure 6 outperforms structure 5 because the order of gold (Au) and silver (Ag) layers in bimetallic SPR sensors has a significant impact on their performance. Below is a comparison of the Prism/Au/Ag and Prism/Ag/Au layouts. Prism/Au/Ag Configuration Greater sensitivity and angular shift can be achieved by placing the Au layer closer to the prism and the Ag layer closer to the sensing medium. The Au layer enhances the plasmonic effect due to its excellent optical properties, while the Ag layer improves overall sensitivity. The sensitivity of structure 6 is 161.81 deg/RIU, with an angular shift of 2.09°. The FOM is determined by the relationship between sensitivity and FWHM according to Eq. (4), so the lower the FOM, the better the performance of the biosensor. We can conclude that structure 6 is better than the structure 5 which it is illustrated by the values in Table 3.

In general, adding a perovskite layer enhances the sensors' sensitivity and FOM. Bimetallic combinations, such as Ag/Au and Au/Ag, also improve sensitivity over single metal layers.

It is concluded that structure 6 has the best sensitivity with a slightly high FOM compared to the other structure. Then, this situation guided us to test its capacity with another type of cell like fibroadenoma, the curves in Fig. 3 indicate the capacity of the suggested sensor to detect fibroadenoma, and the figure illustrates resonance angles between 73.32° and 71.43° corresponding to shift angle equal to 1.89° for normal and fibroadenoma cells respectively. Furthermore, the FWHM presents a low value compared to cancer cells reaching 6.8° and a minimum reflection intensity of 0.007532; this is because the fibroadenoma cells have lower real and imaginary permittivity compared to normal and cancer cells which enhance the sensitivity to the value of 178.63 μs shown in Table 4.

## Conclusion

This work investigated the design and implementation of surface plasmon resonance (SPR) sensors for the sensitive detection of cancer cells in breast tissue. The primary focus was on optimizing the metal layer structure to attain the best sensitivity for distinguishing between normal and malignant cells based on RI differences. The study effectively recognized the importance of optimizing the thickness of silver and gold layers in sensor design. This optimization produced the lowest reflectance and the strongest evanescent field, resulting in increased sensitivity in detecting RI changes. The sensor structure presents the great challenge; it must be carefully fabricated to optimize sensitivity while minimizing noise. This includes selecting optimal materials, configurations and transmission for the prism, the active metal layers by controlling composition and thickness especially at low value like 5 nm, preventing oxidation, and guaranteeing uniformity, as well as the perovskite layer. The study found a striking association between the RI of the sensing media (breast cells) and the resonance angle shift. Cancer cells have a lower RI than normal cells, causing a significant change in the resonance angle. The experiment compared several sensor configurations: The basic Prism/Ag/Sensing medium configuration provided good sensitivity (120.55 deg/RIU) but had a broader resonance peak FWHM, which could affect precision. The Prism/Au/Sensing medium arrangement achieved a better sensitivity (148.52 deg/RIU), but at the expense of a very low reflection minimum due to gold's high-absorption qualities. Bimetallic structures using both Ag and Au layers outperformed single metal designs in terms of FWHM, indicating a sharper resonance peak and potentially superior precision. However, the sensitivity was slightly lower than in the gold-only setup. The most promising findings were obtained by layering a perovskite on top of the bimetallic framework. This arrangement increased sensitivity greatly (up to 162 degrees/RIU) while keeping a good FWHM. The perovskite layer's main contribution is its capacity to lower the imaginary part of the surface plasmon vector, resulting in a sharper resonance peak and perhaps better detection accuracy.

**Table 4** The change in the position of the resonant dip (Δθrés in degrees) is due to a change in the RI of normal and fibroadenoma cells of tow last structures

| | Structural details | Δθrés | Sensitivity | FWHM | FOM |
|---|---|---|---|---|---|
| Structure 6 | Prism/Au/Ag/Perovskite/Sensing medium | 1.89° | 178.63 | 6.8° | 26.26 |

**Acknowledgements** The simulation programme used in this work was produced and created using MATLAB in the laboratory of applied optics at the institute of optics and precision mechanics, and is uploaded on GitHub with the link: https://github.com/ILyes82/surface-plasmons-resnance/blob/main/reflectivity.

**Author Contributions** Habia mohamed ilyes: wrote the manuscript Habia ghania Informations and statistics. Manallah Aissa:reviewed the manuscript. Ayadi khaled: reviewed the manuscript.

**Funding** The authors received no support from any organization for the submitted work. No funding was provided to help in the preparation of this manuscript. There was no funding for this study.

**Data Availability** No datasets were generated or analysed during the current study.

## Declarations

**Ethical Approval** The paper was prepared and approved by all the authors. They are all aware of its contents and approve its submission to the journal. In addition, they state that this manuscript has not been published and that there are no plans to publish it elsewhere.

**Competing Interests** The authors declare no competing interests.

## References

1. Kaur B, Kumar S, Kaushik BK (2021) 2D materials-based fiber optic SPR biosensor for cancer detection at 1550 nm. IEEE Sens J 21(21):23957–23964. https://doi.org/10.1109/JSEN.2021.3110967
2. World Health Organisation (2024) Breast cancer. https://www.who.int/news-room/fact-sheets/detail/breast-cancer. Accessed 13 Mar 2024
3. Chung S, Chandra P, Koo JP, Shim YB (2018) Development of a bifunctional nanobiosensor for screening and detection of chemokine ligand in colorectal cancer cell line. Biosens Bioelectron 100:396–403. https://doi.org/10.1016/j.bios.2017.09.031
4. Azad UP, Chandra P (2023) Handbook of nanobioelectrochemistry: application in devices and biomolecular sensing. Handb Nanobioelectrochemistry Appl Devices Biomol Sens 1–950. https://doi.org/10.1007/978-981-19-9437-1
5. Pavel M et al (2018) Contact inhibition controls cell survival and proliferation via YAP/TAZ-autophagy axis. Nat Commun 9(1). https://doi.org/10.1038/s41467-018-05388-x
6. Chen Z et al (2023) Single cell profiling of female breast fibroadenoma reveals distinct epithelial cell compositions and therapeutic targets. Nat Commun 14(1). https://doi.org/10.1038/s41467-023-39059-3
7. Matiatou M et al (2022) Complex refractive index of freshly excised human breast tissue as a marker of disease. Lasers Med Sci 37(6):2597–2604. https://doi.org/10.1007/s10103-022-03524-0
8. Chadha U et al (2022) Recent progress and growth in biosensors technology: a critical review. J Ind Eng Chem 109:21–51. https://doi.org/10.1016/j.jiec.2022.02.010
9. Wilkirson EC et al (2023) Affinity-based electrochemical sensors for biomolecular detection in whole blood. Anal Bioanal Chem 415(18):3983–4002. https://doi.org/10.1007/s00216-023-04627-5
10. Chauhan N, Saxena K, Tikadar M, Jain U (2021) Recent advances in the design of biosensors based on novel nanomaterials: an insight. Nanotechnology and precision engineering, vol. 4(4). AIP Publishing, LLC. https://doi.org/10.1063/10.0006524
11. Samuel VR, Rao KJ (2022) A review on label free biosensors. Biosens Bioelectron X 11(July):100216. https://doi.org/10.1016/j.biosx.2022.100216
12. Daher MG et al (2022) Detection of basal cancer cells using photodetector based on a novel surface plasmon resonance nanostructure employing perovskite layer with an ultra high sensitivity. Plasmonics 17(6):2365–2373. https://doi.org/10.1007/s11468-022-01727-3
13. Sung H et al (2021) Global cancer statistics 2020: GLOBOCAN estimates of incidence and mortality worldwide for 36 cancers in 185 countries. CA Cancer J Clin 71(3):209–249. https://doi.org/10.3322/caac.21660
14. Yang X, Lin Q, Wang Q (2024) The impact of breast-conserving surgery and modified radical mastectomy on postoperative wound complications in patients with early breast cancer. Int Wound J 21(2). https://doi.org/10.1111/iwj.14685
15. Shellaiah M, Sun KW (2020) Review on sensing applications of perovskite nanomaterials. Chemosensors 8(3). https://doi.org/10.3390/chemosensors8030055
16. Ai B, Fan Z, Wong ZJ (2022) Plasmonic–perovskite solar cells, light emitters, and sensors. Microsystems Nanoeng 8(1). https://doi.org/10.1038/s41378-021-00334-2
17. Baek JW, Kim ID (2023) Advances in perovskite oxides for chemiresistive sensors. Accounts Mater Res 4(12):1108–1120. https://doi.org/10.1021/accountsmr.3c00206
18. Chen S, Lin C (2016) High-performance bimetallic film surface plasmon resonance sensor based on film thickness optimization. Optik (Stuttg) 127(19):7514–7519. https://doi.org/10.1016/j.ijleo.2016.05.085
19. El barghouti M, Akjouj A, Mir A (2022) Performance evaluation of multifunctional SPR bimetallic sensor using hybrid 2D-nanomaterials layers. Optik (Stuttg) 269. https://doi.org/10.1016/j.ijleo.2022.169857
20. Chylek J, Ciprian D, Hlubina P (2024) Optimized film thicknesses for maximum refractive index sensitivity and figure of merit of a bimetallic film surface plasmon resonance sensor. Eur Phys J Plus 139(1). https://doi.org/10.1140/epjp/s13360-023-04798-1
21. Wang Q, Cao S, Gao X, Chen X, Zhang D (2022) Improving the detection accuracy of an ag/au bimetallic surface plasmon resonance biosensor based on graphene. Chemosensors 10(1). https://doi.org/10.3390/chemosensors10010010
22. Ran Y et al (2022) Fiber-optic theranostics (FOT): interstitial fiber-optic needles for cancer sensing and therapy. Adv Sci 9(15). https://doi.org/10.1002/advs.202200456
23. Zhou B, Fan K, Li T, Luan G, Kong L (2023) A biocompatible hydrogel-coated fiber-optic probe for monitoring pH dynamics in mammalian brains in vivo. Sensors Actuators B Chem 380. https://doi.org/10.1016/j.snb.2023.133334
24. Ding L, Gong P, Xu B, Ding Q (2021) An optical fiber sensor based on fluorescence lifetime for the determination of sulfate ions. Sensors (Switzerland) 21(3):1–13. https://doi.org/10.3390/s21030954
25. Jin F, Xu Z, Cao D, Ran Y, Guan BO (2024) Fiber-optic biosensors for cancer theranostics: from in vitro to in vivo. Photonic Sensors 14(4). https://doi.org/10.1007/s13320-024-0706-4
26. Masson JF (2020) Portable and field-deployed surface plasmon resonance and plasmonic sensors. Analyst 145(11):3776–3800. https://doi.org/10.1039/d0an00316f
27. Verma S, Pathak AK, Rahman BMA (2024) Review of biosensors based on plasmonic-enhanced processes in the metallic and metamaterial-supported nanostructures. Micromachines 15(4). https://doi.org/10.3390/mi15040502

28. Mariani S, Minunni M (2014) Surface plasmon resonance applications in clinical analysis. Anal Bioanal Chem 406(9–10):2303–2323. https://doi.org/10.1007/s00216-014-7647-5
29. Kumar VR, Kampan NC, Abd Aziz NH, Teik CK, Shafiee MN, Menon PS (2023) Recent advances in surface plasmon resonance (SPR) technology for detecting ovarian cancer biomarkers. Cancers (Basel) 15(23). https://doi.org/10.3390/cancers15235607
30. Momtahen S, Shokoufi M, Ramaseshan R, Golnaraghi F (2023) Near-infrared handheld probe and imaging system for breast tumor localization. IEEE Can J Electr Comput Eng 46(4):246–255. https://doi.org/10.1109/ICJECE.2023.3259239
31. Vitorino R, Barros AS, Guedes S, Caixeta DC, Sabino-Silva R (2023) Diagnostic and monitoring applications using near infrared (NIR) spectroscopy in cancer and other diseases. Photodiagnosis Photodyn Ther 42. https://doi.org/10.1016/j.pdpdt.2023.103633
32. Coppola F, Frigau L, Markelj J, Malešič J, Conversano C, Strlič M (2023) Near-infrared spectroscopy and machine learning for accurate dating of historical books. J Am Chem Soc 145(22):12305–12314. https://doi.org/10.1021/jacs.3c02835
33. Momtahen S, Momtahen M, Ramaseshan R, Golnaraghi F (2023) An optical sensory system for assessment of residual cancer burden in breast cancer patients undergoing neoadjuvant chemotherapy. Sensors 23(12). 2023. https://doi.org/10.3390/s23125761
34. Wu Y, Feng J, Hu G, Zhang E, Yu HH (2023) Colorimetric sensors for chemical and biological sensing applications. Sensors 23(5). https://doi.org/10.3390/s23052749
35. Yang FQ, Ge L (2023) Colorimetric sensors: methods and applications. Sensors 23(24). https://doi.org/10.3390/s23249887
36. Chowdhury NA, Wang L, Gu L, Kaya M (2023) Exploring the potential of sensing for breast cancer detection. Appl Sci 13(17). https://doi.org/10.3390/app13179982
37. Carneiro MCCG, Rodrigues LR, Moreira FTC, Sales MGF (2022) Colorimetric paper-based sensors against cancer biomarkers. Sensors 22(9). https://doi.org/10.3390/s22093221
38. Duan Y et al (2023) Diagnostic accuracy of optical coherence tomography for margin assessment in breast-conserving surgery: a systematic review and meta-analysis. Photodiagnosis Photodyn Ther 43. https://doi.org/10.1016/j.pdpdt.2023.103718
39. Zeppieri M et al (2023) Optical coherence tomography (OCT): a brief look at the uses and technological evolution of ophthalmology. Med 59(12). https://doi.org/10.3390/medicina59122114
40. Almawgani AHM et al (2023) Sensitivity enhancement of optical plasmon-based sensor for detection of the hemoglobin and glucose: a numerical approach. Opt Quantum Electron 55(11). https://doi.org/10.1007/s11082-023-05219-4
41. Bouzari N, Amjad JM, Mohammadkhani R, Jahanshahi P (2020) Abrupt phase change in graphene-gold spr-based biosensor. Mater Res Express 7(1). https://doi.org/10.1088/2053-1591/ab6d2e
42. El-assar M, Taha TE, El-Samie FEA, Fayed HA, Aly MH (2023) ZnSe-based highly-sensitive SPR biosensor for detection of different cancer cells and urine glucose levels. Opt Quantum Electron 55(1):1–16. https://doi.org/10.1007/s11082-022-04326-y
43. Pandey AK (2020) Plasmonic sensor utilizing Ti3C2Tx MXene layer and fluoride glass substrate for bio- and gas-sensing applications: performance evaluation. Photon Nanostruct - Fundam Appl 42(January):100863. https://doi.org/10.1016/j.photonics.2020.100863
44. Sasivimolkul S, Pechprasarn S, Somekh MG (2021) Analysis of open grating-based Fabry-Pérot resonance structures with potential applications for ultrasensitive refractive index sensing. IEEE Sens J 21(9):10628–10636. https://doi.org/10.1109/JSEN.2021.3063136
45. Singh S, Sharma AK, Lohia P, Dwivedi DK (2021) Optik Theoretical analysis of sensitivity enhancement of surface plasmon resonance biosensor with zinc oxide and blue phosphorus / MoS 2 heterostructure. Optik (Stuttg) 244(July):167618. https://doi.org/10.1016/j.ijleo.2021.167618
46. Sharma AK (2013) Plasmonic biosensor for detection of hemoglobin concentration in human blood: design considerations. J Appl Phys 114(4). https://doi.org/10.1063/1.4816272
47. Yesudasu V, Pradhan HS, Pandya RJ (2021) Recent progress in surface plasmon resonance based sensors: a comprehensive review. Heliyon 7(3):e06321. https://doi.org/10.1016/j.heliyon.2021.e06321
48. Shalabney A, Abdulhalim I (2010) Electromagnetic fields distribution in multilayer thin film structures and the origin of sensitivity enhancement in surface plasmon resonance sensors. Sensors Actuators, A Phys 159(1):24–32. https://doi.org/10.1016/j.sna.2010.02.005
49. Aliqab K, Dave K, Sorathiya V, Alsharari M, Armghan A (2023) Numerical analysis of Phase change material and graphene-based tunable refractive index sensor for infrared frequency spectrum. Sci Rep 13(1):1–17. https://doi.org/10.1038/s41598-023-34859-5
50. Habia MI (2024) Biocapteur optique à resonance. Université Ferhat ABBAS - Sétif 1. [Online]. Available: http://dspace.univ-setif.dz:8888/jspui/handle/123456789/4370. Accessed 3 June 2024